Cellulose (2020) 27:9559–9575
https://doi.org/10.1007/s10570-020-03441-x

ORIGINAL RESEARCH

A reliable hydrophobic/superoleophilic fabric filter for oil–water separation: hierarchical bismuth/purified terephthalic acid nanocomposite

Farshad Beshkar · Masoud Salavati-Niasari · Omid Amiri

Received: 5 April 2020 / Accepted: 3 September 2020 / Published online: 15 September 2020
© Springer Nature B.V. 2020

Abstract In the present work, we developed a simple, eco-friendly, and cost-effective approach to fabricate a recyclable hydrophobic/superoleophilic fabric filter using bismuth nanostructures and purified terephthalic acid (PTA)-based resin. First, different morphologies of bismuth nanostructures such as dendritic, hierarchical, flower and cactus-like were prepared by a facile one-step galvanic displacement method. Afterwards, the coating composition of Bi/PTA mixtures was applied on the surface of fabric filters by a simple hand brushing route. The results indicated that the water and oil contact angles of the modified hydrophobic-superoleophilic fabric filter were about 135° and 0°, respectively. The various oil/water mixtures can be successfully separated by a facile gravity-driven filtration using the as-coated hydrophobic filter with the separation efficiency above 93% and repeatability for at least 10 times. Also, the improved hydrophobic filter showed excellent self-cleaning performance for the removal of surface contaminants. The advantages of scalable production, high efficiency, cost-effective, time saving, sustainable and excellent reusability for the prepared hydrophobic-superoleophilic filter make it to be a potential candidate for oil/water separation and self-cleaning applications.

Keywords Hydrophobic/superoleophilic · Fabric filter · Bismuth nanostructures · Purified terephthalic acid · Oil/water separation · Self-cleaning

F. Beshkar · M. Salavati-Niasari (✉)
Institute of Nano Science and Nano Technology, University of Kashan, P. O. Box. 87317-51167, Kashan, Islamic Republic of Iran
e-mail: salavati@kashanu.ac.ir

O. Amiri
Department of Chemistry, College of Science, University of Raparin, Rania, Kurdistan Region, Iraq

Introduction

In recent years, oily wastewater arising from refinery processes has appeared as a serious environmental problem, which threatens the human, animal and plant health. To address this global issue, various techniques including extraction, filtration, chemical dispersion, in situ burning, biological treatment and superhydrophobic materials, are currently developed to separate nonpolar organic contaminants from water suspensions (Beshkar et al. 2017a, b, c; Subroto et al. 2015; Lu et al. 2016; Pan et al. 2017; Malik et al. 2009; Zhang and Seeger 2011). Among these strategies, membrane filtration with hydrophobicity and oleophilicity properties has demonstrated superior separation efficiency, repeatability, scalability, high mechanical and chemical stability, low energy utilization and so on, in the separation of oil derivatives and nonpolar organic pollutants from aqueous solutions (Zularisam et al. 2006; Zhu et al. 2014; Beshkar

et al. 2020; Mortazavi-Derazkola et al. 2015; Masjedi-Arani and Salavati-Niasari 2016; Ghanbari and Salavati-Niasari 2015; Yousefi et al. 2011; Abbasi et al. 2016).

On the other hand, artificial superhydrophobic surfaces with high water contact angle have widespread applications in oil/water separation, self-cleaning, anti-corrosion, anti-icing, etc. (Yue et al. 2017; Cao et al. 2017a, b; Boinovich et al. 2016). Generally, two stages are employed to fabricate a superhydrophobic surface, i.e., generation of rough surface structure and hydrophobic modification of surface with low surface energy materials (Cheng et al. 2017; Darmanin and Guittard 2014). Therefore, by coating the hierarchical nanostructures combined with hydrophobic modifiers, a rough and superhydrophobic surface can be achieved. Heretofore, different methods have been employed to fabricate the superhydrophobic surfaces including chemical vapor deposition, lithography, chemical etching, sol–gel, electro-spinning, self-assembly, dip-coating, spraying, electro-deposition, and polymerization)Dong et al. 2013; Cao et al. 2017a, b; Ruan et al. 2013; Taurino et al. 2008; Ganesh et al. 2013; Qian et al. 2009; Hao et al. 2012). With the help of the above mentioned methods, a widespread range of materials and surfaces have been applied for the extension of oil–water separation systems like mesh membranes, non-woven textiles and polyurethane sponges, polyester fabrics, aerogels and nanoparticles (Kansara et al. 2016; Piltan et al. 2016).

A variety of work has been reported for the fabrication of various superhydrophobic substrates, like metal, wood, paper, ceramic, textile, and composite substrates (Khattab et al. 2020; Ou et al. 2020). Recently, hydrophobic fabrics have gained great attention due to flexibility, lightness, portability, durability, breathability, affluence, cost-effective, and abundant applications such as membranes, umbrellas, shadow shelters, clothing, textiles and advertising materials (Xu et al. 2020; Patil and Netravali 2020). Textile fabrics are made-up of cellulose and due to the extensive quantities of hydroxyl groups on the cellulose surface, its products are inherently hydrophilic. The construction of superhydrophobic fabric filters by utilizing organic/inorganic composites can be obtained through either physical blending or chemical bonding between hydrophobic organic polymers and inorganic nanoparticles (Sanchez et al. 2011). The artificial superhydrophobic surfaces are based on the principle of manufacturing surface roughness using inorganic micro/nanoparticles such as TiO_2, ZnO, SiO_2, CeO_2, CuO, Ag, and Au, followed by chemical modifications using low surface energy polymers such as fluoroalkylsilane, polydimethylsiloxane, stearic acid, polyacrylate, styrene–butadiene–styrene, polyamide, polytetrafluoroethylene and so on (Khattab et al. 2020; Xu et al. 2020; Patil and Netravali 2020; Beshkar et al. 2017a, b, c; Prasad et al. 2016; Beshkar et al. 2020; Liao et al. 2017). It is worth mentioning that the modified cellulose fabrics have particular functions in smart textiles, including hydrophobicity, anti-UV, conductivity, antibacterial, anti-wrinkle, flame-retardancy and photocatalytic properties (Zanrosso and Lansarin 2019; Kocić et al. 2019; Fallah Moafi et al. 2011).

So far, some works has been done to prepare superhydrophobic metal surfaces such as Au on Cu foil, Pt on Zn film, Ag on Cu substrate, Co micro/nanostructure, nanostructured Ni film, Sn on Zn substrate and so on (Song et al. 2009; Ning et al. 2011; Sarkar and Saleema 2010; Qiu et al. 2011; Gu and Tu 2011; Cao et al. 2013). Moreover, recently bismuth compounds have emerged in some fields including medicine, nontoxic pigment, alloy and chemical industry, photocatalysis, semiconductor and hydrophobicity (Sun et al. 2004; Hu et al. 2015; Leonard et al. 2011; Li et al. 2017; Yan et al. 2015; Yu et al. 2018a, b). Heretofore, only a few reports focused on fabricating hydrophobic bismuth-based surfaces, including BiOCl film, Bi_2WO_6 nanosheets layer, Bi_2S_3 nanostructure, Bi/Bi_2O_3/ZnO surface, Bi nanoparticles, Bi/Bi_2O_3 film, BiOCOOH and $(BiO)_2CO_3$ micro/nanomaterials (Yu et al. 2018a, b; Cao et al. 2014; Yang et al. 2017; Su et al. 2015).

It is well known that fractal structures which are hierarchically self-similar, show interesting properties due to their special physical characteristics related to the fractal dimensions. In particular, hierarchical dendritic nanostructures are one of the most popular structures to synthesis superhydrophobic/superoleophilic surfaces (Su et al. 2015; Feder 1988). It has been reported that galvanic replacement reactions and hand brushing are two efficient methods for the preparation of hierarchical structures and superhydrophobic surfaces owing to their simplicity in equipment and manipulation, mild conditions, morphology-controllable, and facility for the construction

of large-area surfaces (Cao et al. 2014; Alamri et al. 2018).

During the past years, purified terephthalic acid (PTA) compounds, which are made by the reaction between para-xylene and acetic acid, have been widely used as raw materials for fabricating a wide range of products such as high-performance plastics, polyester fiber, resin, film, textile fibers and polyethylene terephthalate bottles. Due to the excellent hardness, anticorrosion, stain resistance and hydrophobicity of the PTA materials, they can be employed as coatings resins to improve the intended properties (Kleerebezem et al. 2005; Verma et al. 2010).

Herein, we developed a simple and low-cost route to produce a durable hydrophobic/superoleophilic fabric filter using hierarchical bismuth nanostructures and purified terephthalic acid (PTA) resin for separating oil derivatives and nonpolar organic solvents from their aqueous mixtures. First, different morphologies of bismuth nanostructures including dendritic, flower, hierarchical and cactus-like were generated by a green, quick and effective galvanic displacement method. Afterwards, the composition of Bi/PTA mixtures were coated on the surface of fabric filters by a simple hand brushing route. The results represented that various oil/water mixtures can be separated by a simple gravity-driven filtration using the modified hydrophobic filter. Also, the improved hydrophobic filter showed excellent self-cleaning activity for the removal of surface contaminants. The advantages of scalable production, high efficiency, cost-effective, time saving, sustainable and excellent reusability for the as-fabricated hydrophobic-superoleophilic filter enable it to be an outstanding candidate for self-cleaning and oil/water separation usages.

Experimental

Materials and methods

All chemicals were purchased from Merck Company and used without purification. Gasoline was purchased from Esfahan Oil Refining Company, Isfahan, Iran. Also, purified terephthalic acid (PTA)-based resin was purchased from Vikram Resins and Polymers Company, Bengaluru, Karnataka, India. X-ray diffraction (XRD) analysis was measured by a Philips-X'PertPro, X-ray diffractometer using Cu-Kα radiation ($\lambda = 0.15418$ nm). Scanning electron microscopy (SEM) images were taken on Hitachi S-4160. Fourier transform infrared (FT-IR) analysis was measured via Magna-IR, spectrometer 550 Nicolet in KBr pellets in the range of 400–4000 cm^{-1}. Water and oil contact angles were evaluated using a contact-angle meter (Veho USB microscope 400x, china) equipped with a CCD camera at room temperature. Transmission electron microscopy (TEM) and High-Resolution TEM (HRTEM) images were obtained on a JEM-2100 with an accelerating voltage of 200 kV.

Synthesis of Bismuth nanostructures

Various morphologies of bismuth nanostructures were fabricated by a facile and simple galvanic replacement reaction. In a typical synthesis, first zinc foil was immersed in 6 M HCl aqueous solution for 20 min to remove zinc oxide layer followed by washing with distilled water and dried at room temperature. Afterward, cleaned foil was immersed in aqueous solution of $Bi(NO_3)_3.5H_2O$ containing 1 mL of concentrated HNO_3. Also, different surfactants including PEG600, Triton X100 and SDBS with mole ratio of 1:1 to bismuth salt were used. Final products were rinsed three time with distilled water and ethanol, then dried in a vacuum oven at 70 °C. The production details of bismuth nanostructures are presented at Table 1.

Preparation of hydrophobic fabric filter

First, a piece of commercial fabric filter was cleaned with 6 M HCl aqueous solution and dried in an oven at 70 °C for 30 min. On the other hand, 1 g of as-prepared bismuth nanostructures were dispersed in 10 g of purified terephthalic acid (PTA) resin after 20 min of ultrasonication. Subsequently, the obtained mixtures were coated on the fabric filter surfaces utilizing a facile and effective one-step hand-brushing procedure. Finally, the modified filter samples were cured at 70 °C in an oven for 1 h. Figure 1 shows the un-coated fabric filter (left) and as-modified hydrophobic fabric filter (right).

Table 1 Details of the synthesis and water contact angles of bismuth nanostructures

Sample no.	Concentration of $Bi(NO_3)_3{\cdot}5H_2O$ (mM)	Time (s)	Surfactant	Morphology	Water contact angle (°)
1	4	60	–	Rod	118
2	20	60	–	Dendritic	133
3	40	60	–	Sheet	115
4	20	10	–	Spherical	112
5	20	150	–	Hole	121
6	20	60	PEG-600	Hierarchical	135
7	20	60	Triton X100	Cactus	127
8	20	60	SDBS	Flower	119

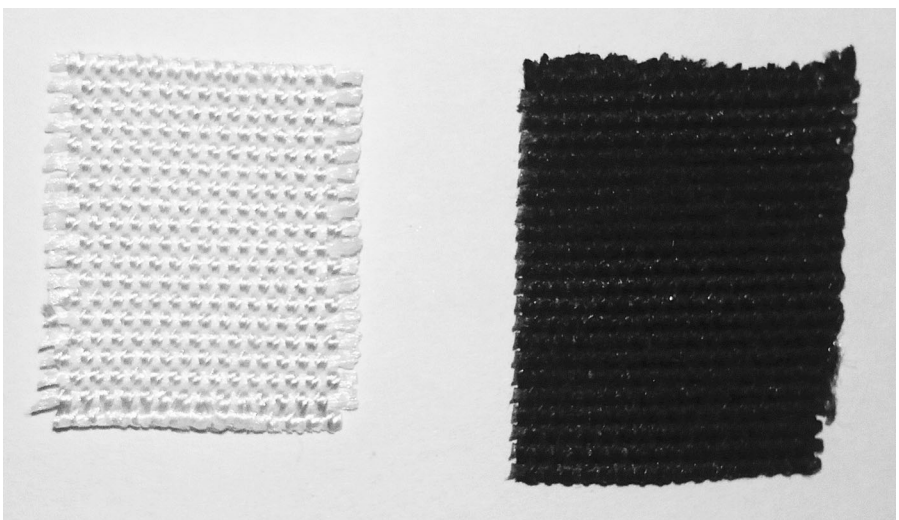

Fig. 1 The color change of the fabric filter: (left) un-coated and (right) coated fabric filter by hierarchical Bi nanostructures and PTA resin

Oil/water separation performance of hydrophobic fabric filter

In order to appraise the oil/water separation proficiency of the optimized hydrophobic fabric filter, five artificial oily solvents containing various oils of gasoline, decane, petroleum ether, toluene and hexane were employed. In a typical experiment, 20 mL of gasoline and water mixture with volume ratio of 1:1 was employed as oil/water mixture. The water was colored by methylene blue dye. The as-modified hydrophobic fabric filter was applied as a filter membrane, which was put in a 3-way distillation adapter of the round-bottom flask. The gasoline/water mixture was dropped onto the hydrophobic filter. The gasoline fell into the flask, while the water dropped into the cylinder. The separation efficiency (SE) of the as-coated hydrophobic fabric filter was computed according to the following equation:

$$SE = \frac{W\alpha}{W\beta} * 100\,(\%) \quad (1)$$

where W_β is the weight of oil before separation, and W_α is the penetration weight of oil after filtration.

Result and discussion

X-ray diffraction (XRD) measurement was used to determine the phase composition and crystallinity of the as-prepared bismuth sample. Figure 2a shows the XRD pattern of the sample no. 2. As seen in the

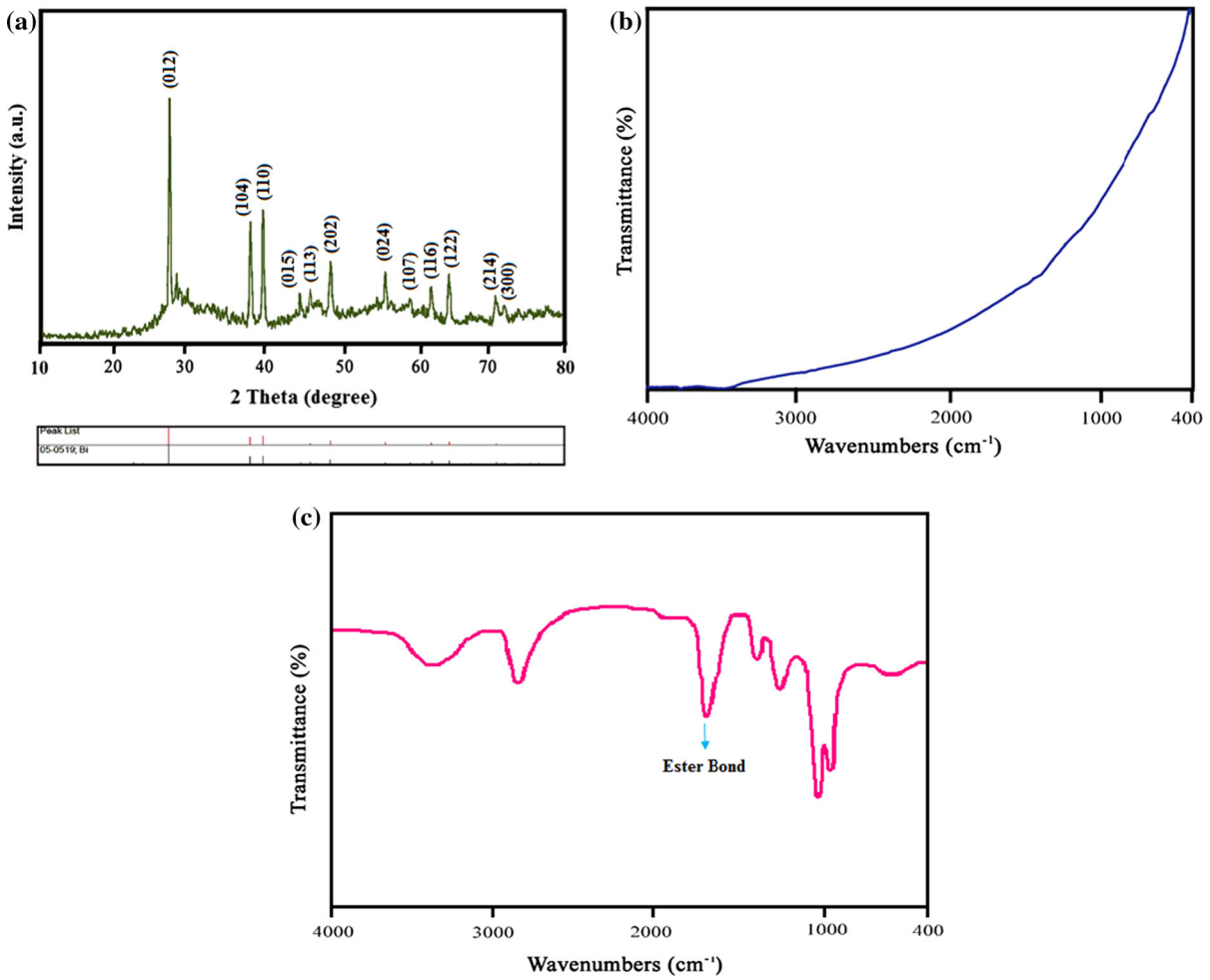

Fig. 2 **a** The XRD pattern, **b** FTIR spectrum of the dendritic-like bismuth nanostructures and **c** FTIR spectra of the modified fabric filter by Bi/PTA nanocomposite

Fig. 2a, XRD pattern completely matched with the standard reference card of elemental Bi (JCPDS No. 05-0519). According to the XRD results, prepared bismuth nanostructures have rhombohedral crystal system with R-3 m space group. The broad and sharp diffraction peaks indicate that the bismuth nanostructures have high crystalline phase with the average crystal size about 24 nm. Moreover, we recognized no diffraction peaks of any other impurities, which exhibits the high purity of the product. In addition, FT-IR analysis was employed to investigate the surface functional groups of bismuth nanostructures. Figure 2b illustrates the FTIR spectrum of the as-synthesized bismuth nanostructure (sample no. 2). As seen from the FTIR spectrum, there is no transmittance peaks for the elemental bismuth nanostructure that shows the preparation method, washing and drying processes were effective. To further verify of modification of the fabric filter, the FT-IR analysis of treated fabric by Bi/PTA nanocomposite was taken and illustrated in Fig. 2c. It is obvious that the esteric bonds can be formed between carboxylic groups of PTA and hydroxyl groups of cellulose chains of fabrics. As shown in FT-IR spectrum, the characteristic peaks at around 1075, 1448, 2919 and 3420 cm^{-1} are attributed to the C–O stretching, CH_2 symmetric bending, C–H stretching and O–H stretching of cellulose, respectively (Xu et al. 2015; Wulandari et al. 2016). It is reported that the characteristic peaks of carboxyl groups in PTA are located at about 1680 cm^{-1} (C=O) and 1280 cm^{-1} (C–O), whereas, the peak of carbonyl groups in esters emerges at

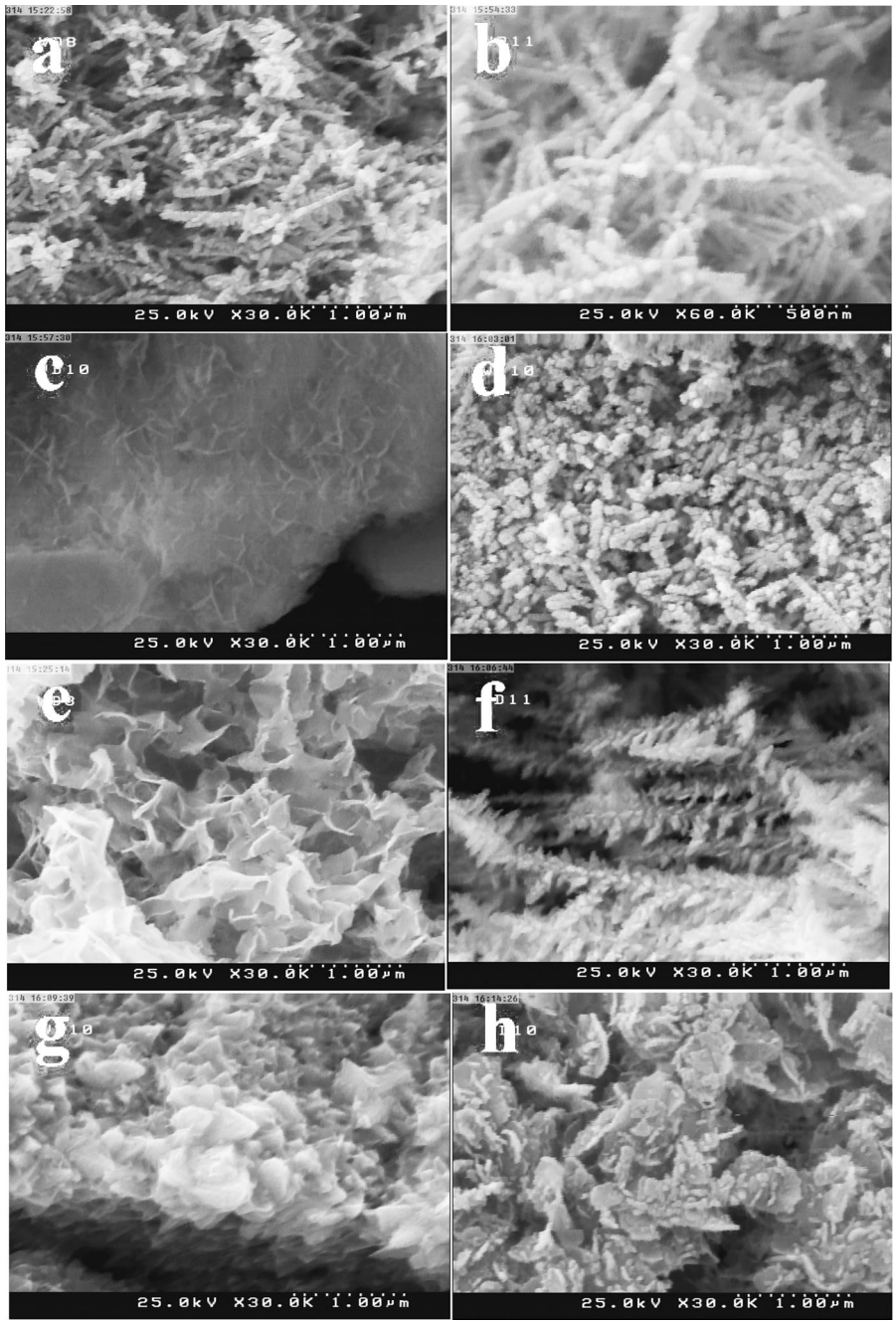

Fig. 3 **a–h** The SEM images of the various morphologies of bismuth micro/nanostructures (sample nos. 1–8), respectively, prepared by galvanic replacement approach

around 1720 cm^{-1}. Therefore, the transmittance peak at 1740 cm^{-1} can be ascribed to the asymmetric stretching vibrations of ester carbonyl groups, which indicates that the PTA has formed covalent ester bonds with cellulose polymer on the fabrics. As well as, the peak at 1296 cm^{-1} can be assigned to the C–O stretching of PTA compound (Fig. 2a–c) (Zhao et al. 2018; Khajavi and Berendjchi 2014; Zhou et al. 2019). On the other hand, the as-created polymeric network can surround and immobilize the bismuth

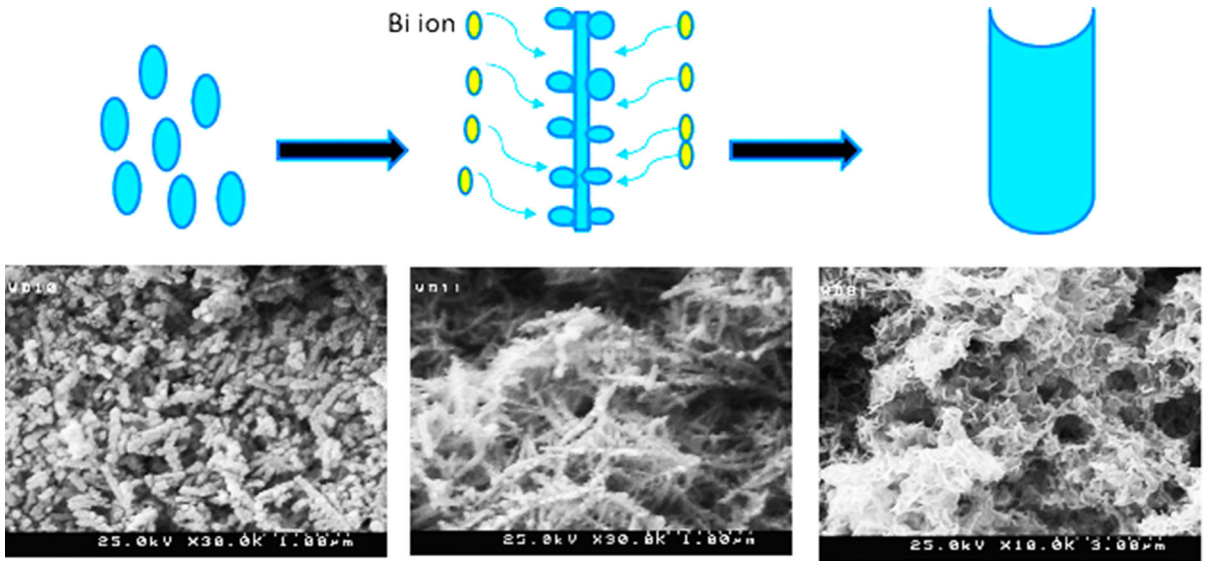

Scheme 1 Possible mechanism for the effect of the reaction time on the morphology of bismuth products

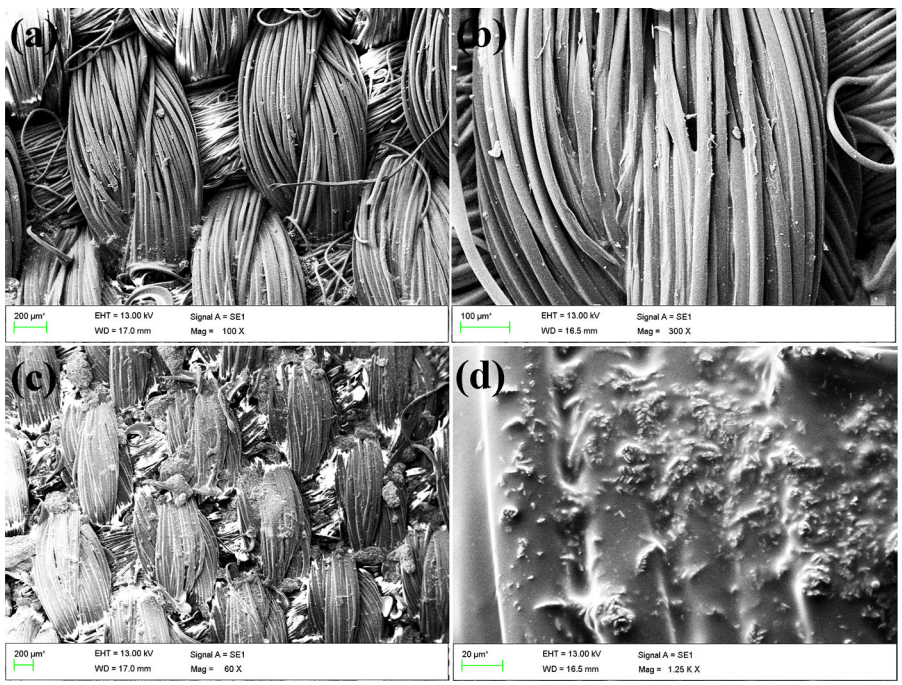

Fig. 4 The SEM images of **a**, **b** pristine fabric filter and **c**, **d** modified fabric filter by dendritical Bi-PTA sample

nanostructures onto the fabric surface (as shown in Fig. 4c) and thus, a durable hydrophobic fabric filter can be achieved.

Herein, various morphologies of bismuth nanostructures were prepared by a novel and real fast galvanic replacement method. Bismuth nanostructures can be prepared in a few seconds at room temperature. During the replacement reaction, Zn atoms are oxidized to Zn^{2+} ions and subsequently, Bi^{3+} ions can be reduced to the Bi element. We also engineered morphology of final products by changing the reaction conditions. Particle size and morphology of a

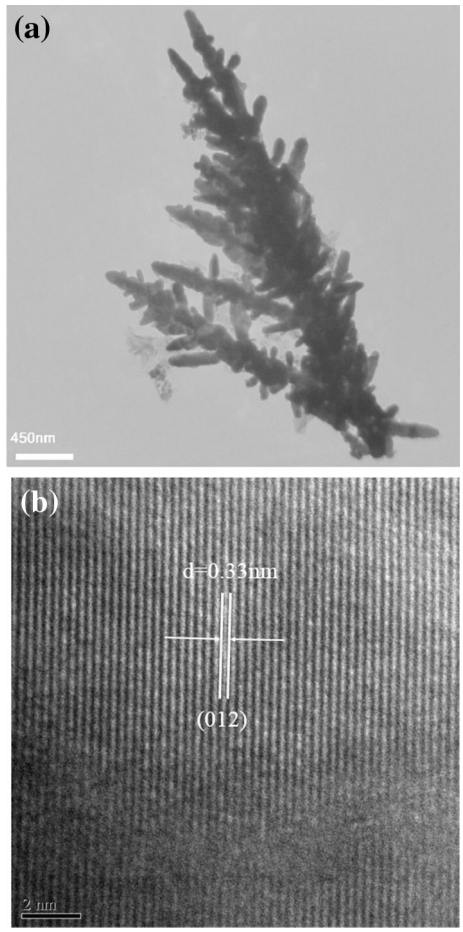

Fig. 5 **a** The TEM and **b** HRTEM images of the as-prepared dendritic-like bismuth nanostructure (sample no. 2)

nanostructure have significant effect on its properties and performances (Beshkar et al. 2017a, b, c; Namvar et al. 2017).

Concentration of bismuth precursor is an important parameter which impacts on the final morphology of the Bi products. In this case, by fixing the reaction time at 60 s, when the concentration of $Bi(NO_3)_3{\cdot}5H_2O$ was 4 mM (sample no. 1), rod-like nanostructures were achieved (Fig. 3a). According to the Fig. 3b, c, by increasing the concentration to 20 mM (sample no. 2), dendritic-like bismuth nanostructure were obtained (Fig. 3b), while raising the concentration to 40 mM (sample no. 3) lead to form sheet-like bismuth nanostructures (Fig. 3c).

Another important parameter is reaction time of galvanic replacement process. Herein, three different times (10, 60 and 150 s) were studied at constant concentration (20 mM). Figure 3d, e illustrate the influence of the reaction time on the shape of final samples. As seen in Fig. 3d, the reaction time (10 s) was not enough to form the dendritic nanostructures (sample no. 4). In this time, initial nuclear of bismuth was formed. By increasing the reaction time to 60 s, dendritic nanostructures were formed (Fig. 3b). It seems that, by increasing the reaction time to 60 s, primary particles of bismuth had enough time to growth and form the fractal structures. In other words, the arrangement of Bi dendrites was compatible with the situation of orientated formation of as-prepared Bi nanoparticles. When the reaction time was extended further to 150 s (sample no. 5), more bismuth ions was reduced and filled the free spaces between the branches in sample no. 2, and finally the hole-like nanostructures were achieved (see Fig. 3e and Scheme 1) (Cao et al. 2014).

Figure 3f–h represent the SEM images of bismuth structures fabricated in the presence of various surfactants (PEG600, Triton X100, and SDBS) at concentration of 20 mM and reaction time for 60 s. It is evident that the hierarchical nanostructures (Fig. 3f), cactus-like structures (Fig. 3g) and flower-like micro/nanostructures (Fig. 3h) were prepared utilizing PEG600 (sample no. 6), Triton X100 (sample no. 7) and SDBS (sample no. 8), respectively. As observed, the interesting morphologies of bismuth samples were achieved by changing the type of surfactant. The various morphologies of Bi structures can be attributed to the high value of defect sites/vacancies, steric hindrance and the selective reaction on specific facets arising from the surfactant effect (Cobley and Xia 2010; Najafian et al. 2019).

Moreover, as we know the wettability phenomena depends on the morphological structure of the surface. As illustrated in Fig. 4a, b, the pristine fabric filter is fabricated by the uniform intertwined bunches of very smooth fibers. In addition, the SEM images of the treated fabric filter by Bi/PTA nanocomposites were displayed in Fig. 4c, d. It is obvious that the as-coated fabric filter by hierarchical Bi micro/nanostructures (sample no. 6) and PTA resin demonstrates high roughness at both the micro-and nano-scales. By depositing the Bi/PTA coatings on the fabrics surface, the hierarchical Bi micro/nanostructures were randomly dispersed on the surface and constructed the valleys and hills upon the fabrics surface. As well as, it is clear that the PTA resin can uniformly stick to the

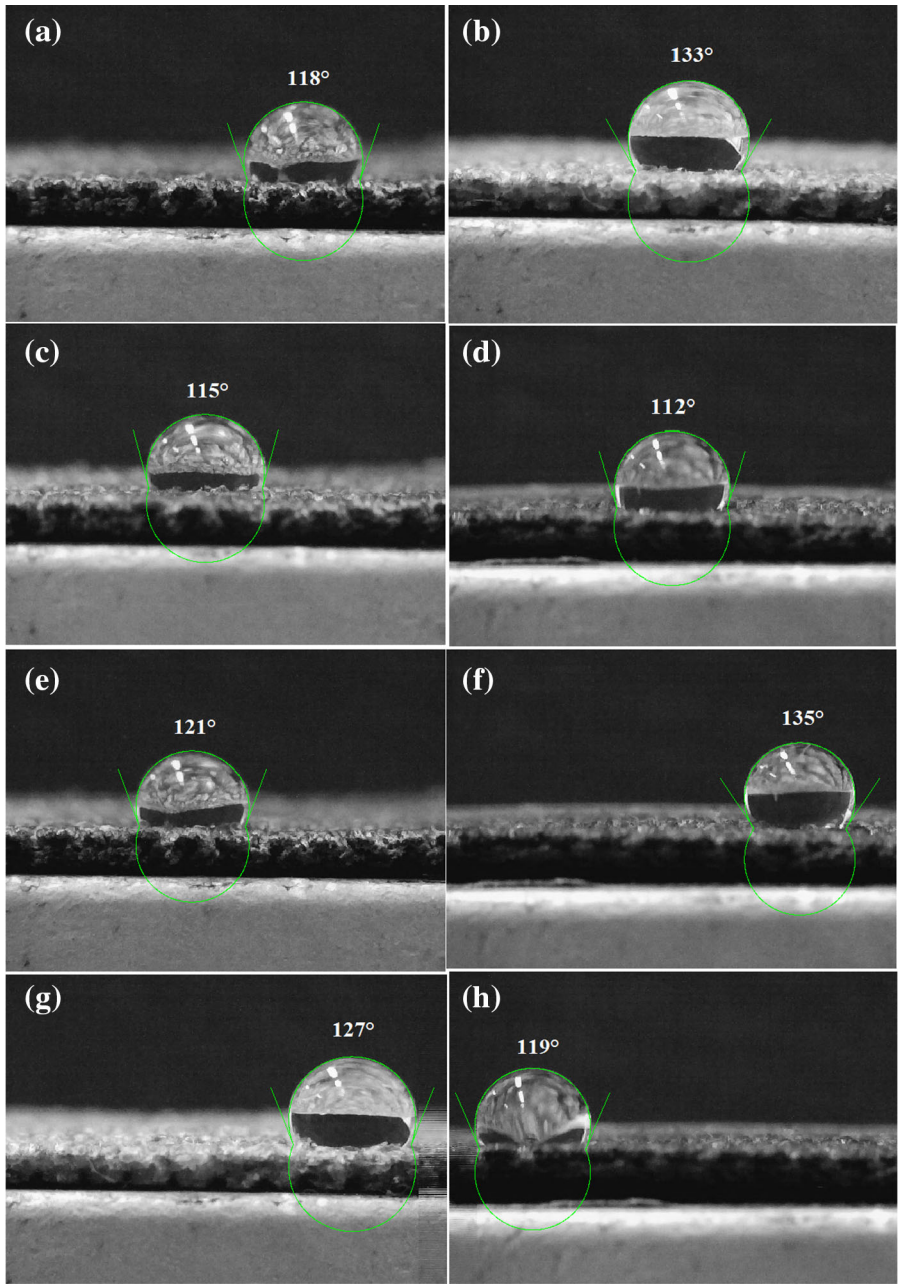

Fig. 6 **a–h** Water contact angle images of the fabric filters modified by various morphologies of bismuth micro/nanostructures (sample nos. 1–8, respectively) and PTA resin

fabrics surface, and improve the adhesion between the Bi structures and fabrics. Ultimately, by incorporating of the Bi-based roughness and the layer of PTA resin, the treated fabric filter represents relatively hydrophobicity with the WCA of 135° (Fig. 6f). This observation approves that creating the optimal surface roughness on a substrate is essential for improving its hydrophobicity.

The detailed length of the stem and side branch of the dendritic-like bismuth nanostructure (sample no. 2) was evaluated by transmission electron microscopy (TEM). The TEM image (Fig. 5a) displays that the

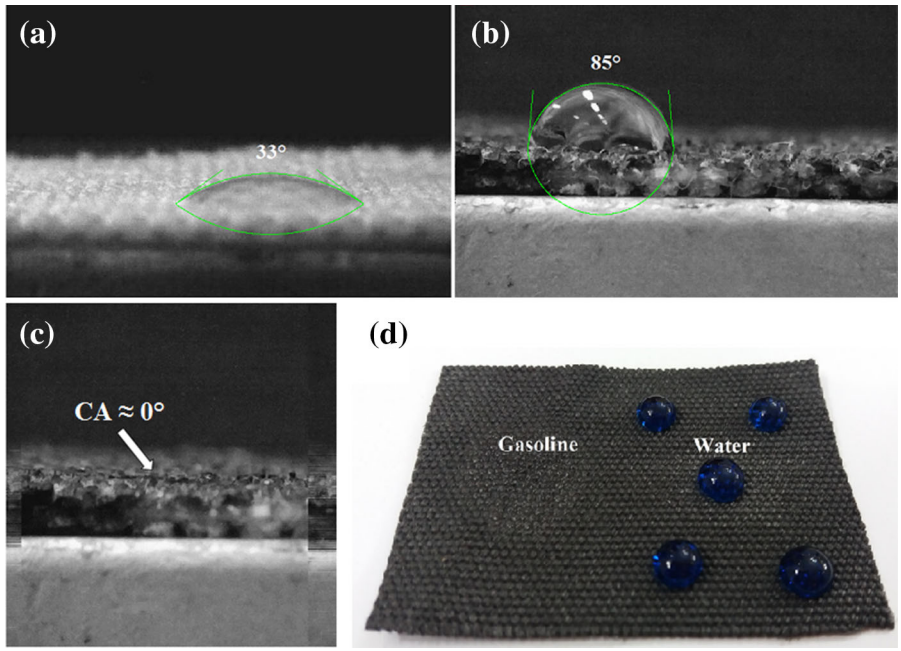

Fig. 7 Micrographs of the contact angles for the water droplets on the surface of the **a** pristine fabric filter, **b** purified terephthalic acid resin-coated filter and **c** the gasoline droplet on the surface of the as-coated filter and **d** the graphical illustration for the surface hydrophobicity-superoleophilicity of the modified filter toward water and gasoline droplets

bismuth structures have dendritic-like shape which the length of the Bi stem along the axis can be as long as 4 µm and the diameter is about 200 nm, whereas the length of its side branches is around 50 nm. Also, the detailed structure information of sample no. 2 was further appraised by high-resolution transmission electron microscopy (HRTEM). As shown in Fig. 5b, the interlayer distance of 0.33 nm correspond to the (012) lattice plane of hierarchical bismuth nanostructures, which was in accordance with the XRD data.

As we know the geometrical structure and chemical composition of a surface can characterize its wettability properties. Also, both the surface roughness and surface functional groups modification induced the surface to have considerable hydrophobicity/oleophilicity properties, because the plentiful air trapped in the water/substrate interfaces can suspend the water droplet upon the surface (Beshkar et al. 2017a, b, c; Cao et al. 2016). Therefore, it is anticipated that as-coated fabric filter with particular hierarchical micro/nanostructures may result in a remarkable hydrophobicity. The wetting properties of the as-prepared hydrophobic fabric filters were evaluated by water contact angle (WCA) measurements. The various morphologies of bismuth micro/nanostructures were employed to increase the surface roughness of the filters. The results of WCAs analysis of the sample nos. 1–8 are depicted in Fig. 6a–h and Table 1. As can be seen, all prepared bismuth samples enhanced the hydrophobicity of the filters. Among them, the dendritic-like (sample no. 2) and hierarchical (sample no. 6) shapes exhibited the higher hydrophobicity effect with water contact angles about 133° and 135°, respectively (Fig. 6b, f). It is evident that as-produced hierarchical bismuth architectures with special micro/nanostructures can lead to a notable hydrophobicity of the filter. As hierarchical Bi micro/nanostructures deposited on the filter surface, the membrane surface became rough because the branch porous structures scattered well over the surface, and these particular micro/nanostructures are similar to the protrusions on the lotus leaf surface (Fan et al. 2019). As well as, the hierarchical structures, which are rough on both micro- and nanoscale (so called micro-nano-binary structures) can minimize the contact area of the air trapped between the solid surface and the water droplet, and finally enhance the hydrophobicity of the surface (Khranovskyy et al. 2012).

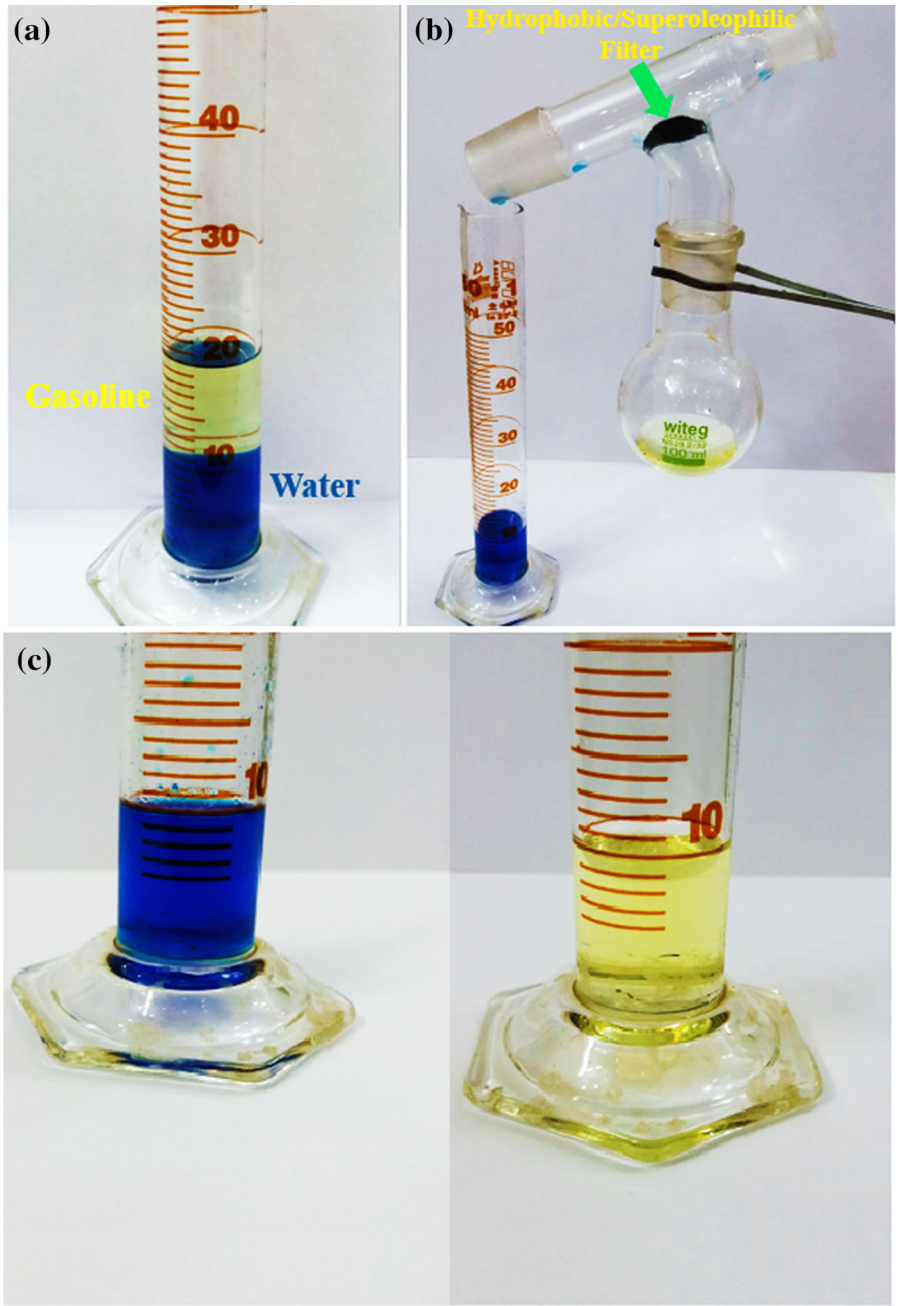

Fig. 8 Graphical illustration of oil–water separation experiment by optimized hydrophobic fabric filter (**a**–**c**). The water was colored by methylene blue dye

Moreover, Fig. 7a, b, illustrate the micrographs of the water droplet on the surface of the pristine fabric filter and purified terephthalic acid resin-coated filter, respectively. As can be seen, for the pristine and resin-coated filters, the corresponding WCAs are determined to be 33° and 85°, respectively, which indicate that they have hydrophilic effect and need to be further modified to gain the hydrophobicity property. The hydrophobicity and oleophilicity properties of a filter are two chief factors for the oil/water separation application. It is reported that the textile filters are potential candidates for oil/water separation due to

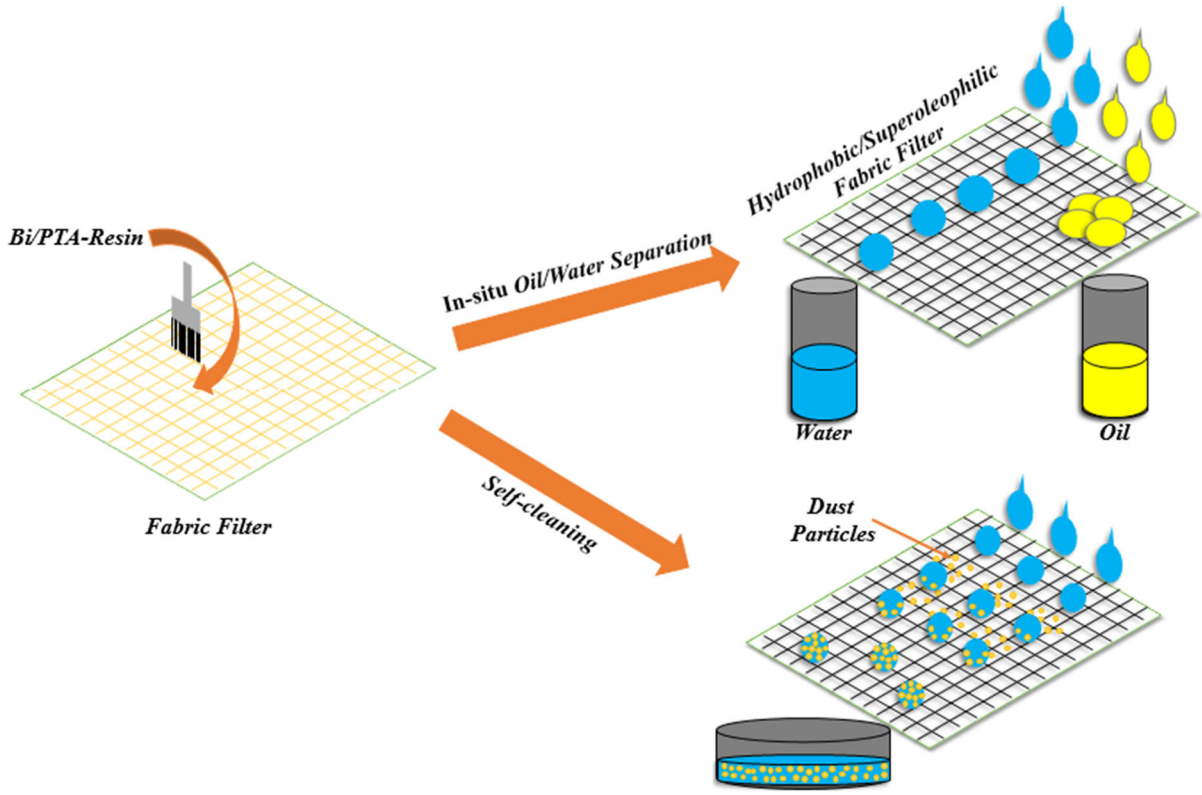

Scheme 2 Schematic design for the fabrication of the hydrophobic bismuth/PTA-resin-based fabric filter and its oil/water separation and self-cleaning performances

their selectivity, softness, flexibility, reusability and endurance (Kansara et al. 2016; Li et al. 2012; Lim and Huang 2006). As can be seen in Figs. 6f and 7c, the bismuth/resin-coated filter exhibited hydrophobicity with the water contact angle of 135° and superoleophilicity with the oil contact angle of 0°, which causes the water droplets slip from the filter surface, while allowing the oil droplets (in this case gasoline) to permeate through the filter quickly (Fig. 7d). Therefore, the oil–water separation tests were performed utilizing the as-prepared hydrophobic fabric filter under gravity-driven separation system. When the gasoline–water mixture was poured onto the hydrophobic filter, gasoline easily infiltrated through the filter and rapidly dropped into the flask below. On the other hand, water droplets could not penetrate through the filter and thus was poured into the cylinder below (Fig. 8a–c). After filtration, only pure and transparent gasoline was observed which exhibits the excellent oil–water separation activity of the as-modified hydrophobic fabric filter. Scheme 2 demonstrates the schematic design of the fabrication of the hydrophobic/superoleophilic fabric filter by bismuth nanostructures and PTA resin and its performance for the oil/water separation and self-cleaning.

Moreover, the separation performance of the other oily solvents by optimized hydrophobic filter are shown in Fig. 9a. As illustrated in Fig. 9a, the separation efficiencies of the fabricated hydrophobic filter with hierarchical bismuth/resin layers for various oil–water mixtures were all above 93%, especially for gasoline it was about 98%. The facile, time saving, high separation efficiency and gravity-driven oil/water separation of the hydrophobic/superoleophilic filter can provide more chances for widespread industrial applications. As well known, for industrial oil cleanup utilizations, the recyclability of the membrane and recovery of the oils or organic solvents characterizes its service lifetime and large scale application value (Jin et al. 2015). Recycle test of the as-obtained hydrophobic/superoleophilic filter was also carried out for 10 times of gasoline/water separation to investigate

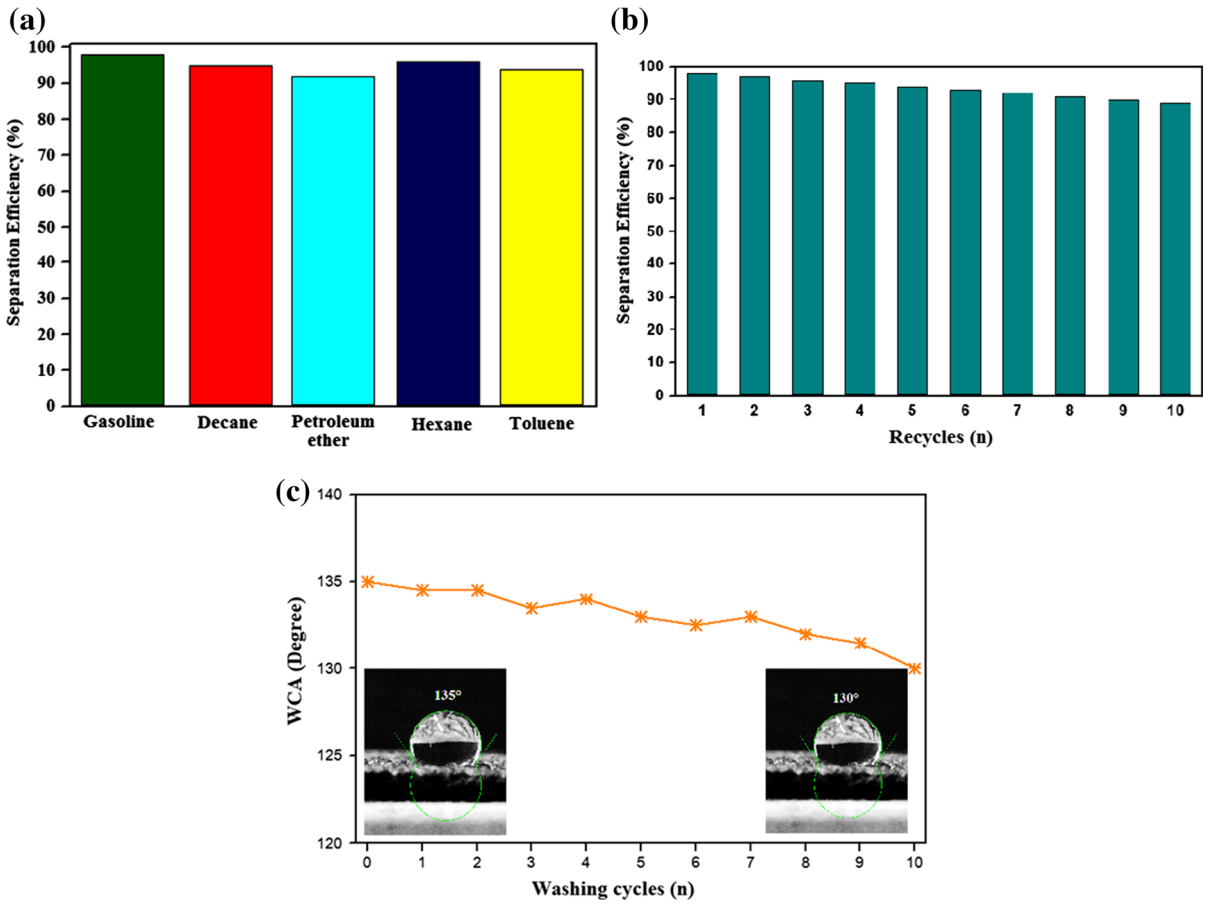

Fig. 9 **a** The separation performance of the various oil–water mixtures, **b** the recycle test of the as-fabricated hydrophobic filter for 10 times of gasoline/water separation and **c** the stability test of the modified hydrophobic filter after recycling and washing processes

Table 2 A comparison of typical examples for various types of oil/water separation materials

Separation materials	Separated compound	WCA (°)	Separation efficiency (%)	Refs.
Polydivinylbenzene-coated cotton fabric	Silicon oil	147	98	Cheng et al. (2019)
TiO_2/vinyl trimethoxysilane-coated cotton fabric	Oil free air compressor	150	98	He et al. (2020)
Bi-coated iron mesh	hexane	163	96	Yu et al. (2018a, b)
Cu–graphite/SBS-based cotton filter	Gas condensates	152	94	Beshkar et al. (2020)
Bi/PTA-based fabric filter	Gasoline	135	93	This work

the reusability of our filter. Oil separation efficiency remained constant even after 10 consecutive cycles without significant change in the oil separation performance as illustrated in Fig. 9b. Even after 10 times of repetition, the hierarchical bismuth/resin-coated filter still exhibited superior separation efficiency of gasoline as about 98%, indicating that the as-prepared hydrophobic filter is stable and reusable. Furthermore, the stability of the hydrophobicity feature of the bismuth/PTA-coated fabric filter was

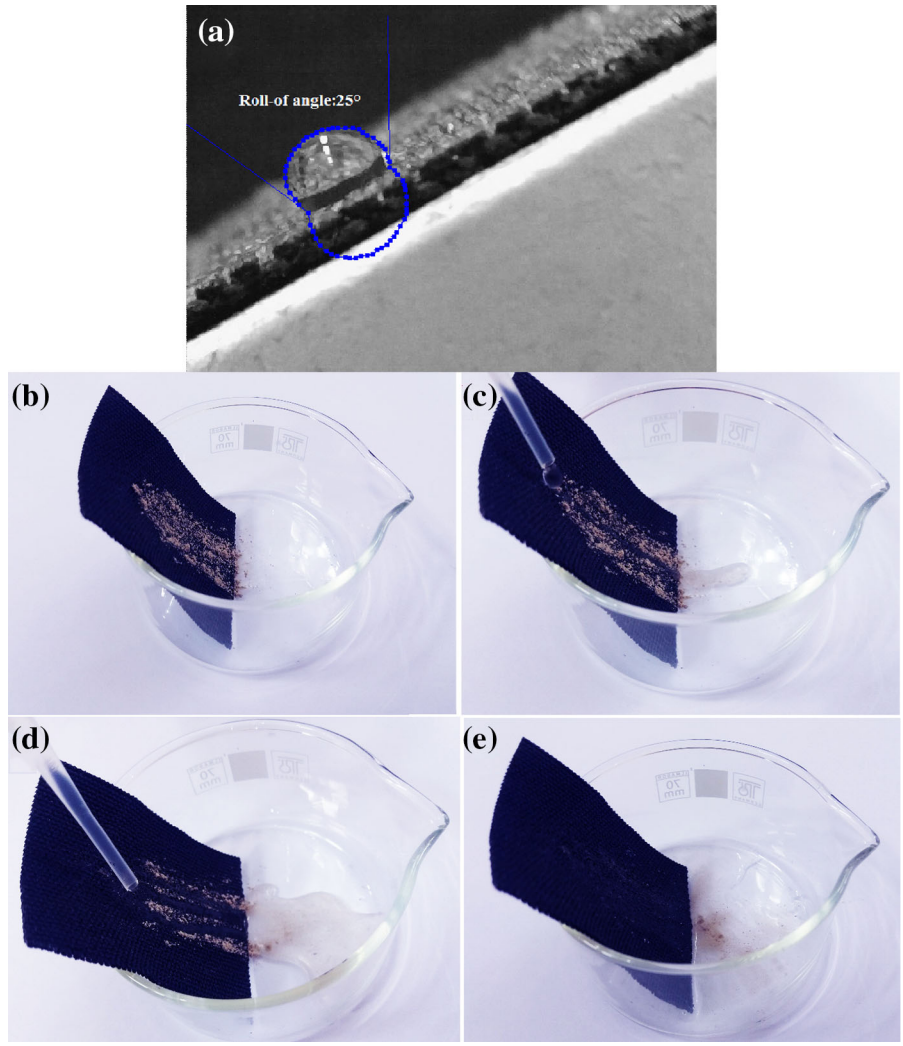

Fig. 10 **a** Roll-off angle of the optimized hydrophobic filter and **b–e** the self-cleaning performance of the as-modified filter by rolling the water droplets on the surface to remove the dust powder

evaluated by washing and recycling of the as-modified filter for 10 runs and the change in WCA was recorded. As demonstrated in Fig. 9c, the hydrophobic filter exhibited excellent hydrophobicity with WCA of around 130° after 10 cycles of washing and reusing. This result can be ascribed to the good affinity between the bismuth/PTA composites and fabric filter.

A broad range of oil/water separation compounds has been evaluated in the previous literatures. Here, for a better comparison, some typical oil/water separation compounds are listed in Table 2. As can be seen, the separation performance of our-synthesized Bi/PTA-based fabric filter is almost similar to the performance of other reported materials, but it can be stated that our-modified filter has been obtained by a facile fabrication process, inexpensive cost, eco-friendly, favorable absorption properties and large scale production.

The hydrophobic surfaces with low water adhesion commonly possess the potential for self-cleaning applications. In the self-cleaning effect, water droplets can easily roll off the substrate and passingly remove the contaminants on its surface. As observed, the micro/nano-protrusions formed by hierarchical Bi structures created the uniform valleys and hills over fabric surface, which leads to the generation of more air pockets on the surface and subsequently lowest contact area between water droplet and surface (Fan

et al. 2019). Figure 10a demonstrated that the roll-off angle of the modified hydrophobic filter was about 25°, indicating the coated filter can be used as a self-cleaning material. The self-cleaning activity of the hydrophobic hierarchical bismuth/resin-modified filter was investigated, as shown in Fig. 10b–e. Dust was applied as a target pollutant which was sprinkled on the surface of tilted filter, and after that the filter surface was rinsed with water droplets. It could be clearly seen in Fig. 10b–e, when water droplets touched the surface, they immediately rolled down the hydrophobic filter surface and took dust particles away. Finally, as shown in Fig. 10e, the fabric surface was taken out from the dirt after several water drops, verifying the modified filter has a good non-wetting characteristic and can be employed for self-cleaning applications.

Conclusion

In summary, the hydrophobic/superoleophilic fabric filter was fabricated based on bismuth nanostructures and PTA resin utilizing a green and simple brushing approach. Various morphologies of bismuth nanostructures such as hierarchical, dendritic, cactus and flower-like were prepared by controlling the galvanic displacement reaction parameters such as type of surfactant, reaction time and concentration of bismuth precursor. When the hydrophobic/superoleophilic covering was put on the surface of fabric filter, the modified membrane demonstrated high separation efficiencies with values greater than 93% during the separation of various oil/water mixtures. Also, reusability evaluation of the as-prepared hydrophobic filter showed good repeatability for at least 10 times of the gasoline/water separation. Moreover, the modified hydrophobic filter exhibited excellent self-cleaning activity for the elimination of the surface pollutants. The results indicate that the as-fabricated hydrophobic/superoleophilic filter can be employed for the efficient oil/water separation and self-cleaning performance for industrial-scale applications.

Acknowledgments Authors are grateful to the council of Iran National Science Foundation (97017837) and University of Kashan for supporting this work by Grant No. (159271/897790).

References

Abbasi A, Ghanbari D, Salavati-Niasari M, Hamadanian M (2016) Photo-degradation of methylene blue: photocatalyst and magnetic investigation of Fe_2O_3–TiO_2 nanoparticles and nanocomposites. J Mater Sci Mater Electron 27(5):4800–4809

Alamri H, Al-Shahrani A, Bovero E, Turki K, Alabedi G, Obaid W, Al-Taie I, Fihri A (2018) Self-cleaning superhydrophobic epoxy coating based on fibrous silica-coated iron oxide magnetic nanoparticles. J Colloid Interface Sci 513:349–356

Beshkar F, Amiri O, Salehi Z (2017a) Synthesis of $ZnSnO_3$ nanostructures by using novel gelling agents and their application in degradation of textile dye. Sep Purif Technol 184:66–71

Beshkar F, Khojasteh H, Salavati-Niasari M (2017b) Flower-like CuO/ZnO hybrid hierarchical nanostructures grown on copper substrate: glycothermal synthesis, characterization, hydrophobic and anticorrosion properties. Materials 10:697

Beshkar F, Khojasteh H, Salavati-Niasari M (2017c) Recyclable magnetic superhydrophobic straw soot sponge for highly efficient oil/water separation. J Colloid Interf Sci 497:57–65

Beshkar F, Salavati-Niasari M, Amiri O (2020) Superhydrophobic–superoleophilic copper–graphite/styrene–butadiene–styrene based cotton filter for efficient separation of oil derivatives from aqueous mixtures. Cellulose 27:4691–4705

Boinovich LB, Emelyanenko AM, Emelyanenko KA, Maslakov KI (2016) Anti-icing properties of a superhydrophobic surface in a salt environment: an unexpected increase in freezing delay times for weak brine droplets. Phys Chem Chem Phys 18:3131–3136

Cao L, Liu J, Huang W, Li ZL (2013) Facile fabrication of superhydrophobic surfaces on zinc substrates by displacement deposition of Sn. Appl Surf Sci 265:597–602

Cao L, Lu X, Pu F, Yin X, Xia Y, Huang W, Li Z (2014) Facile fabrication of superhydrophobic Bi/Bi_2O_3 surfaces with hierarchical micro-nanostructures by electroless deposition or electrodeposition. Appl Surf Sci 288:558–563

Cao MY, Guo DW, Yu CM, Li K, Liu MJ, Jiang L (2016) Water-repellent properties of superhydrophobic and lubricant-infused slippery surfaces: a brief study on the functions and applications. ACS Appl Mater Interfaces 8:3615–3623

Cao WT, Liu YJ, Ma MG, Zhu JF (2017a) Facile preparation of robust and superhydrophobic materials for self-cleaning and oil/water separation. Colloids Surf A 529:18–25

Cao N, Yang B, Barras A, Szunerits S, Boukherroub R (2017b) Polyurethane sponge functionalized with superhydrophobic nanodiamond particles for efficient oil/water separation. Chem Eng J 307:319–325

Cheng QY, An XP, Li YD, Huang CL, Zeng JB (2017) Sustainable and biodegradable superhydrophobic coating from epoxidized soybean oil and ZnO nanoparticles on cellulosic substrates for efficient oil/water separation. ACS Sustain Chem Eng 5:1440–11450

Cheng QY, Guan CS, Li YD, Zhu J, Zeng JB (2019) Robust and durable superhydrophobic cotton fabrics via a one-step

solvothermal method for efficient oil/water separation. Cellulose 26:2861–2872
Cobley CM, Xia Y (2010) Engineering the properties of metal nanostructures via galvanic replacement reactions. Mater Sci Eng R 70:44–62
Darmanin T, Guittard F (2014) Recent advances in the potential applications ofbioinspired superhydrophobic materials. J Mater Chem A 2:16319–16359
Dong J, Yao ZH, Yang TZ, Jiang LL, Shen CM (2013) Control of superhydrophilic and superhydrophobic graphene interface. Sci Rep 3:1733
Fallah Moafi H, Fallah Shojaie A, Zanjanchi MA (2011) Flame-retardancy and photocatalytic properties of cellulosic fabric coated by nano-sized titanium dioxide. J Therm Anal Calorim 104:717–724
Fan T, Miao J, Li Z, Cheng B (2019) Bio-inspired robust superhydrophobic-superoleophilic polyphenylene sulfide membrane for efficient oil/water separation under highly acidic or alkaline conditions. J Hazard Mater 373:11–22
Feder J (1988) Fractals. Plenum Press, New York
Ganesh VA, Dinachali SS, Raut HK, Walsh TM, Nair AS, Ramakrishna S (2013) Electrospun SiO_2 nanofibers as a template to fabricate a robust and transparent superamphiphobic coating. RSC Adv 3:3819–3824
Ghanbari D, Salavati-Niasari M (2015) Synthesis of urchin-like CdS-Fe_3O_4 nanocomposite and its application in flame retardancy of magnetic cellulose acetate. J Ind Eng Chem 24:284–292
Gu CD, Tu JP (2011) One-step fabrication of nanostructured Ni film with lotus effect from deep eutectic solvent. Langmuir 27:10132–10140
Hao LM, Chen Z, Wang RP, Guo CL, Zhang PL, Pang SF (2012) A non-aqueous electrodeposition process for fabrication of superhydrophobic surface with hierarchical micro/nano structure. Appl Surf Sci 258:8970–8973
He T, Zhao H, Liu Y, Zhao C, Wang L, Wang H, Zhao Y, Wang H (2020) Facile fabrication of superhydrophobic titanium dioxide-composited cotton fabrics to realize oil-water separation with efficiently photocatalytic degradation for water-soluble pollutants. Colloids Surf A Physicochem Eng Asp 585:124080
Hu ZT, Liu J, Yan X, Oh WD, Lim TT (2015) Low-temperature synthesis of graphene/$Bi_2Fe_4O_9$ composite for synergistic adsorption-photocatalytic degradation of hydrophobic pollutant under solar irradiation. Chem Eng J 262:1022–1032
Jin Y, Jiang P, Ke Q, Cheng F, Zhu Y, Zhang Y (2015) Superhydrophobic and superoleophilic polydimethylsiloxane-coated cotton for oil–water separation process: an evidence of the relationship between its loading capacity and oil absorption ability. J Hazard Mater 300:175–181
Kansara AM, Chaudhri SG, Singh PS (2016) A facile one-step preparation method of recyclable superhydrophobic polypropylene membrane for oil-water separation. RSC Adv 6:61129–61136
Khajavi R, Berendjchi A (2014) Effect of dicarboxylic acid chain length on the self-cleaning property of nano-TiO_2-coated cotton fabrics. ACS Appl Mater Interfaces 6:18795–18799
Khattab TA, Mohamed AL, Hassabo AG (2020) Development of durable superhydrophobic cotton fabrics coated with silicone/stearic acid using different cross-linkers. Mater Chem Phys 249:122981
Khranovskyy V, Ekblad T, Yakimova R, Hultman L (2012) Surface morphology effects on the light-controlled wettability of ZnO nanostructures. Appl Surf Sci 258:8146–8152
Kleerebezem R, Beckers J, Hulshoff Pol LW, Lettinga G (2005) High rate treatment of terephthalic acid production wastewater in a two-stage anaerobic bioreactor. Biotechnol Bioeng 91:169–179
Kocić A, Bizjak M, Popović D, Poparić GB, Stanković SB (2019) UV protection afforded by textile fabrics made of natural and regenerated cellulose fibres. J Clean Prod 228:1229–1237
Leonard NM, Wieland LC, Mohan RS (2011) Applications of bismuth (III) compounds in organic synthesis. Cheminform 40:4649–4707
Li J, Shi L, Chen Y, Zhang Y, Guo Z, Su BL, Liu W (2012) Stable superhydrophobic coatings from thiol-ligand nanocrystals and their application in oil/water separation. J Mater Chem 22:9774–9781
Li YH, Sun Y, Cao TY, Su QQ, Li ZL, Huang MX, Ouyang RZ, Chang HZ, Zhang SP, Miao YQ (2017) A cation-exchange controlled core-shell MnS@Bi_2S_3 theranostic platform for multimodal imaging guided radiation therapy with hyperthermia boost. Nanoscale 9:14364–14375
Liao R, Li C, Yuan Y, Duan Y, Zhuang A (2017) Anti-icing performance of ZnO/SiO_2/PTFE sandwich-nanostructure superhydrophobic film on glass prepared via RF magnetron sputtering. Mater Lett 206:109–112
Lim TT, Huang X (2006) In situ oil/water separation using hydrophobic–oleophilic fibrous wall: a lab-scale feasibility study for groundwater cleanu. J Hazard Mater B 137:820–826
Lu DW, Zhang T, Gutierrez L, Ma J, Croue JP (2016) Influence of surface properties of filtration-layer metal oxide on ceramic membrane fouling during ultrafiltration of oil/water emulsion. Environ Sci Technol 50:4668–4674
Malik AA, Ahmad J, Mir SR, Ali M, Abdin MZ (2009) Influence of chemical and biological treatments on volatile oil composition of *Artemisia annua* Linn. Ind Crop Prod 30:380–383
Masjedi-Arani M, Salavati-Niasari M (2016) A simple sonochemical approach for synthesis and characterization of Zn_2SiO_4 nanostructures. Ultrason Sonochem 29:226–235
Mortazavi-Derazkola S, Zinatloo-Ajabshir S, Salavati-Niasari M (2015) Novel simple solvent-less preparation, characterization and degradation of the cationic dye over holmium oxide ceramic nanostructures. Ceram Int 41(8):9593–9601
Najafian H, Manteghi F, Beshkar F, Salavati-Niasari M (2019) Fabrication of nanocomposite photocatalyst $CuBi_2O_4$/Bi_3ClO_4 for removal of acid brown 14 as water pollutant under visible light irradiation. J Hazard Mater 361:210–220
Namvar F, Beshkar F, Salavati-Niasari M, Bagheri S (2017) Morphology-controlled synthesis, characterization and photocatalytic property of hierarchical flower-like $Dy_2Mo_3O_9$ nanostructures. J Mater Sci Mater Electron 28:10313–10320
Ning T, Xu WG, Lu SX (2011) One-step controllable fabrication of superhydrophobic surfaces with special composite

structure on zinc substrates. J Colloid Interf Sci 361:388–396
Ou J, Wang F, Li W, Yan M, Amirfazli A (2020) Methyltrimethoxysilane as a multipurpose chemical for durable superhydrophobic cotton fabric. Prog Org Coat 146:105700
Pan Z, Zhao L, Boufadel MC, King T, Robinson B, Conmy R, Lee K (2017) Impact of mixing time and energy on the dispersion effectiveness and droplets size of oil. Chemosphere 166:246–254
Patil NV, Netravali AN (2020) Bioinspired process using anisotropic silica particles and fatty acid for superhydrophobic cotton fabrics. Cellulose 27:545–559
Piltan S, Seyfi J, Hejazi I, Davachi SM, Khonakdar HA (2016) Superhydrophobic filter paper via an improved phase separation process for oil/water separation: study on surface morphology, composition and wettability. Cellulose 23:3913–3924
Prasad G, Chakradhar RPS, Bera P, Anand Prabu A, Anandan C (2016) Transparent hydrophobic and superhydrophobic coatings fabricated using polyamide 12–SiO_2 nanocomposite. Surf Interface Anal 49:427–433
Qian Z, Zhang ZC, Song LY, Liu HR (2009) A novel approach to raspberry-like particles for superhydrophobic materials. J Mater Chem 19:1297–1304
Qiu R, Zhang D, Wang P, Zhang XL, Kang YS (2011) Tunable electrochemical preparation of cobalt micro/nanostructures and their morphology-dependent wettability property. Electrochim Acta 58:699–706
Ruan M, Li W, Wang BS, Deng BW, Ma FM, Yu ZL (2013) Preparation and anti-icing behavior of superhydrophobic surfaces on aluminum alloy substrates. Langmuir 29:8482–8491
Sanchez C, Belleville P, Popall M, Nicole L (2011) Applications of advanced hybrid organic-inorganic nanomaterials: from laboratory to market. Chem Soc Rev 40:696–753
Sarkar DK, Saleema N (2010) One-step fabrication process of superhydrophobic green coatings. Surf Coat Technol 204:2483–2486
Song W, Zhang JJ, Xie YF, Cong Q, Zhao B (2009) Large-area unmodified superhydrophobic copper substrate can be prepared by an electroless replacement deposition. J Colloid Interf Sci 329:208–211
Su C, Lu Z, Zhao H, Yang H, Chen R (2015) Photoinduced switchable wettability of bismuth coating with hierarchical dendritic structure between superhydrophobicity and superhydrophilicity. Appl Surf Sci 353:735–743
Subroto E, Manurung R, Heeres HJ, Broekhuis AA (2015) Mechanical extraction of oil from *Jatropha curcas* L. kernel: effect of processing parameters. Ind Crops Prod 63:301–310
Sun H, Zhang L, Szeto KY (2004) Bismuth in medicine. Met Ions Biol Syst 41:333–378
Taurino R, Fabbri E, Messori M, Pilati F, Pospiech D, Synytska A (2008) Facile preparation of superhydrophobic coatings by sol–gel processes. J Colloid Interf Sci 325:149–156
Verma S, Prasad B, Mishra IM (2010) Pretreatment of petrochemical wastewater by coagulation and flocculation and the sludge characteristics. J Hazard Mater 178:1055–1064
Wulandari WT, Rochliadi A, Arcana IM (2016) Nanocellulose prepared by acid hydrolysis of isolated cellulose from sugarcane gagasse. IOP Conf Ser Mater Sci Eng 107:012045
Xu LL, Guo MX, Liu S, Bian SW (2015) Graphene/cotton composite fabrics as flexible electrode materials for electrochemical capacitors. RSC Adv 5:25244–25249
Xu LH, Pan H, Wang LM, Shen Y, Ding Y (2020) Preparation of fluorine-free superhydrophobic cotton fabric with polyacrylate/SiO_2 nanocomposite. J Nanosci Nanotechnol 20:2292–2300
Yan T, Yan Q, Wang X, Liu H, Li M, Lu S, Xu W, Sun M (2015) Facile fabrication of heterostructured g-C_3N_4/Bi_2MoO_6 microspheres with highly efficient activity under visible light irradiation. Dalton Trans 44:1601–1611
Yang H, Hu X, Su C, Liu Y, Chen R (2017) Reversibly photoswitchable wettability of stearic acid monolayer modified bismuth-based micro-/nanomaterials. Phys Chem Chem Phys 19:31666–31674
Yousefi M, Gholamian F, Ghanbari D, Salavati-Niasari M (2011) Polymeric nanocomposite materials: preparation and characterization of star-shaped PbS nanocrystals and their influence on the thermal stability of acrylonitrile–butadiene. Polyhedron 30(6):1055–1060
Yu T, Lu S, Xu W (2018a) A reliable filter for oil-water separation: bismuth coated superhydrophobic/superoleophilic iron mesh. J Alloys Compd 769:576–587
Yu T, Lu S, Xu W, He G (2018b) Fabrication of bismuth superhydrophobic surface on zinc substrate. J Solid State Chem 262:26–37
Yue XJ, Zhang T, Yang DY, Qiu FX, Rong J, Xu JC, Fang JS (2017) The synthesis of hierarchical porous Al_2O_3/acrylic resin composites as durable, efficient and recyclable absorbents for oil/water separation. Chem Eng J 309:522–531
Zanrosso CD, Lansarin MA (2019) Application of polycarboxylic acids as binders for TiO_2 immobilization on cotton textiles. Braz J Chem Eng 36:181–190
Zhang JP, Seeger S (2011) Polyester materials with superwetting silicone nanofilaments for oil/water separation and selective oil absorption. Adv Funct Mater 21:4699–4704
Zhao X, Chen H, Chen X, Hu J, Wu T, Wu L, Li M (2018) Multiple halide anion doped layered bismuth terephthalate with excellent photocatalysis for pollutant removal. RSC Adv 8:38370–38375
Zhou J, Hu XY, Zhu YY, Lyu HF, Zhang L, Fu FY, Liu XD (2019) A hybrid binder of carboxymethyl chitosan and L-methionine enables a slight amount of Ag NPs to be durably effective on antibacterial cotton fabrics. Cellulose 26:9323–9333
Zhu Y, Wang D, Jiang L, Jin J (2014) Recent progress in developing advanced membranes for emulsified oil/water separation. NPG Asia Mater 6:e101
Zularisam AW, Ismail AF, Salim R (2006) Behaviours of natural organic matter in membrane filtration for surface water treatment. Desalination 194:211–231

Publisher's Note Springer Nature remains neutral with regard to jurisdictional claims in published maps and institutional affiliations.